Wu Zhao-Qiu (Orcid ID: 0000-0002-0662-2375)

LW106, A Novel Inhibitor of IDO1, Suppresses Tumor Progression by Limiting Stroma-Immune Crosstalk and Cancer Stem Cell Enrichment in the Tumor Microenvironment

Rong Fu[1,†], Yi-Wei Zhang[1,†], Hong-Mei Li[1,2,†], Wen-Cong Lv[1], Li Zhao[1], Qing-Long Guo[1], Tao Lu[2], Stephen J Weiss[3], Zhi-Yu Li[4], Zhao-Qiu Wu[1,*]

[1]State Key Laboratory of Natural Medicines, Jiangsu Key Laboratory of Carcinogenesis and Intervention, School of Basic Medicine and Clinical Pharmacy, China Pharmaceutical University, Nanjing 211198, China; Collaborative Innovation Center for Gannan Oil-Tea Camellia Industrial Development, Gannan Medical University, Ganzhou 341000, China

[2]Laboratory of Molecular Design and Drug Discovery, School of Science, China Pharmaceutical University, Nanjing 211198, China

[3]The Life Sciences Institute, Comprehensive Cancer Center, Division of Molecular Medicine and Genetics, Department of Internal Medicine, University of Michigan, Ann Arbor 48109, USA

[4]Department of Medicinal Chemistry, School of Pharmacy, China Pharmaceutical University, Nanjing 211198, China

[†]These authors contributed equally to this work.

[*]**Corresponding author:** Zhao-Qiu Wu, State Key Laboratory of Natural Medicines, China Pharmaceutical University, Nanjing 211198, China. Phone/Fax: 86-25-86185653; E-mail: zqwu@cpu.edu.cn.

Key words: IDO1, LW106, T cells, non-hematopoietic stromal cells, cancer stem cells

Running title: Targeting IDO1 Limits Stroma-Immune Crosstalk

This is the author manuscript accepted for publication and has undergone full peer review but has not been through the copyediting, typesetting, pagination and proofreading process, which may lead to differences between this version and the Version of Record. Please cite this article as doi: 10.1111/bph.14351

Abstract

Background and Purpose

Indoleamine 2,3-dioxygenase 1 (IDO1) is emerging as an important new therapeutic target for treatment of malignant tumors characterized by dysregulated tryptophan metabolism. However, the antitumor efficacy of existing small-molecule inhibitors of IDO1 is still unsatisfactory and the underlying mechanism remains largely undefined. Hence, we discovered a novel potent small-molecule inhibitor of IDO1, LW106, and studied its antitumor effects and the underlying mechanisms in two Tumor models.

Experimental Approach

C57BL6 mice, athymic nude mice or *Ido1*$^{-/-}$ mice were inoculated with IDO1-expressing and -nonexpressing tumor cells and treated with vehicle, epacadostat or increasing doses of LW106. Xenografted Tumors, plasmas, spleens and other vital organs were harvested and subjected to kynurenine/tryptophan measurement and flow cytometric, histological and immunohistochemical analyses.

Key Results

LW106 dose-dependently inhibited outgrowth of xenografted tumors that were inoculated in C57BL6 mice but not nude mice or *Ido1*$^{-/-}$ mice, showing a stronger antitumor efficacy than epacadostat, an existing IDO1 inhibitor. LW106 substantially elevated intratumoral infiltration of proliferative T_{eff} cells while reduced recruitment of proliferative T_{reg} cells and non-hematopoietic stromal cells such as endothelial cells and cancer-associated fibroblasts. LW106 treatment resulted in a reduced subpopulation of cancer stem cells (CSCs) in xenografted tumors in which less proliferative/invasive tumor cells and more apoptotic tumor cells were observed.

Conclusion and Implications

LW106 inhibits tumor outgrowth by limiting stroma-immune crosstalk and CSC enrichment in the tumor microenvironment. LW106 can be further developed as a potential immunotherapeutic agent used in combination with immune checkpoint

inhibitors and (or) chemotherapeutic drugs for cancer treatment.

Abbreviations: Cancer-associated fibroblasts, CAFs; cancer-associated macrophages, CAMs; cancer stem cells, CSCs; dendritic cells, DCs; distant-metastasis-free survival, DMFS; Dulbecco's modified eagle medium, DMEM; extra cellular matrix, ECM; fetal bovine serum, FBS; hematoxylin and eosin, H&E; human peripheral blood mononuclear cells, PBMCs; human recombinant granulocyte macrophage colony stimulating factors, hGM-CSF; human recombinant interferon γ, hIFN-γ; human recombinant interleukin 4, hIL-4; indoleamine 2,3-dioxygenase 1, IDO1; lipopolysaccharide, LPS; 1-methyl-trytophan, 1-MT; non-small cell lung cancer, NSCLC; not significant, N.S.; overall survival, OS; paraformaldehyde, PFA; post-progression survival, PPS; radio immunoprecipitation assay, RIPA; short tandem repeat, STR; α-smooth muscle actin, α-SMA; specific-pathogen-free, SPF; Tumor microenvironment, TME.

Introduction

The intracellular enzyme indoleamine 2,3-dioxygenase 1 (IDO1) is a monomeric oxidoreductase that catalyzes the first and rate-limiting step in tryptophan degradation, leading to subsequent production of bioactive tryptophan metabolites kynurenine (Botting, 1995; Sono *et al.*, 1980; Sono *et al.*, 1996). IDO1 has been proposed as a potential contributor to immunosuppression, tolerance and tumor escape (Munn *et al.*, 2004; Munn *et al.*, 2007; Munn *et al.*, 1999; Prendergast *et al.*, 2008). IDO1-mediated depletion of tryptophan and production of kynurenine can lead to an immunosuppressive tumor microenvironment (TME), in which the proliferation of effector T cells is inhibited while suppressive populations of regulatory T cells are activated (Munn *et al.*, 2004; Munn *et al.*, 2007; Fallarino *et al.*, 2002; Frumento *et al.*, 2002). The presence of IDO1 in TME has been shown to correlate with tumor progression, invasion and metastasis and can be used as an independent prognostic marker of survival in various types of cancers (Brandacher *et al.*, 2006; Ino *et al.*, 2008; Pan *et al.*, 2008; Polak *et al.*, 2007). It has been demonstrated that IDO1 is produced mainly by the tumor cells and host-derived immune cells such as dendritic cells (DCs) and macrophages that are recruited to TME by the tumor (Munn *et al.*, 1999; Munn *et al.*, 2002).

The TME is the cellular microenvironment in which the tumor exists, including tumor-infiltrating immune cells (*e.g.* T cells, DCs and macrophages) and non-hematopoietic stromal cells such as cancer-associated fibroblasts (CAFs), endothelial cells and pericytes, along with the extracellular matrix (ECM) and inflammatory mediators they secret (Coussen *et al.*, 2002; Hanahan *et al.*, 2011; Hanahan *et al.*, 2012; Johansson *et al.*, 2008; Turley *et al.*, 2015). Emerging evidence suggests that the crosstalk (interaction) between stromal compartment and immune system within the TME can influence tumor growth, metastasis and chemoresistance (Holmgaard *et al.*, 2013; Joyce *et al.*, 2009). CAFs, the predominant stromal cells, together with endothelial cells and pericytes, enhance proliferation, extravasation and infiltration of regulatory T cells and reduce the trafficking of proliferative effector T cells to the tumor bed, which can hinder antitumor immune responses and then promote tumor progression (Buckanovich *et al.*, 2008; Castermans *et al.*, 2007; Feig *et al.*, 2013; Tan *et al.*, 2011; Turley *et al.*, 2015). ECM, the non-cellular component in the TME, may also suppress antitumor immune response and then support tumor growth by limiting T cell motility (Caruana *et al.*, 2015; Provenzano *et al.*, 2012; Salmon *et al.*, 2012; Turley *et al.*, 2015). However, the stromal immunoregulation in the TME is not unidirectional. A growing body of evidence now exists to suggest that the infiltrating immune cells can actively shape the stromal milieu in the TME, thus highlights a considerable level of crosstalk (interaction) between stromal and immune cells (Beatty *et al.*, 2011; Coussens *et al.*, 2013; Lu *et al.*, 2011; Turley *et al.*, 2015). Stromal cells and their associated ECM have been recognized to play an essential role in controlling expansion of cancer stem cells (CSCs), a population tumor cells that possess the defining features of clonogenicity and self-renewal, and CSCs are proposed to have a critical role in tumor progression, metastasis and chemoresistance (Bhowmich *et al.*, 2004; Ni *et al.*, 2016; Turley *et al.*, 2015).

It is still unclear whether tumor cell-derived IDO1 contributes to tumor progression in patients (Holmgaard *et al.*, 2013). In the present study, we perform a bioinformatic analysis for the relationship between tumor cell-derived *IDO1* expression levels and survival rates in patients using an online tool (http://kmplot.com/analysis/), which is capable to assess the effect of 54,675 genes on survival using 10,461 cancer samples, including 5,143 breast, 1,816 ovarian, 2,437 lung and 1,065 gastric cancer patients with

a mean follow-up of 69, 40, 49 and 33 months, respectively (Gyorffy *et al.*, 2010, 2012, 2013; Szasz *et al.*, 2016).

IDO1 is emerging as an important new therapeutic target for the treatment of cancer, and three small-molecule inhibitors of IDO1, 1-methyl-tryptophan (1-MT), NLG919 and epacadostat are currently in clinical trials for treatment of non-small cell lung cancer (NSCLC), melanoma and other types of cancer (Cady *et al.*, 1991; Jackson *et al.*, 2013; Liu *et al.*, 2010). However, the antitumor efficacy of these existing inhibitors is still unsatisfactory and the underlying mechanism remains largely undefined. In the present study, we describe the discovery and characterization of LW106, a structurally novel small-molecule inhibitor of IDO1. We find that LW106 displays a stronger antitumor efficacy as compared with epacadostat, and further reveal that LW106 inhibits tumor growth by limiting the interaction (crosstalk) between stromal compartment and immune system and the enrichment of CSCs in the TME. Our data suggest that LW106 can be further developed as a potential immunotherapeutic agent for cancer treatment.

Materials and Methods

Mice and human samples

Eight-week-old male C57BL/6 mice and athymic nude mice were purchased from Qinglongshan Animal Facility in Nanjing, China. Congenic *Ido1*$^{-/-}$ mice on C57BL/6 strain background were obtained from the Jackson Laboratory. All mice were housed under standard specific-pathogen-free (SPF) conditions and all research involving animals strictly complied with protocols approved by the Animal Welfare and Ethics Committee (AWEC, China Pharmaceutical University). Human peripheral blood mononuclear cells (PBMCs) from healthy volunteers were purchased from Nanjing Red Cross Blood Center.

Chemical compounds

LW106 (MW: 245; Suppl. Fig. 1) was synthesized at the Department of Medicinal Chemistry, School of Pharmacy, China Pharmaceutical University, and the purity was no less than 99%. With the binding model of the lead compound 62 with IDO1 (PDB code: 2D0T) by molecular docking, we probe the active site and discover more potent IDO inhibitors based on 62. It was observed oximido of 62 could interact with heme 7-propionic acid to form a conserved hydrogen contributing greatly to the strong protein

occupancy. The oxadiazole of 62 is directed toward the backup hydrophobic pocket (Arg231, Phe226) and forms a strong cation−π interaction with Arg231 of the protein. While the benzyl group of 62 is oriented toward the small hydrophobic pocket, away from the heme iron and thus lacking any specific interaction with the protein. We hypothesized that replacement of the imine (62) with heterocycles (LW106) to occupy the deep space and stable the conformation of the compound might have a favorable contribution to the affinity improvement. Epacadostat was purchased from MedChem Express. Stock solutions were prepared in DMSO for use in cell-based assays.

Nomenclature of Targets and Ligands

Key protein targets and ligands in this article are hyperlinked to corresponding entries in http://www.guidetopharmacology.org, the common portal for data from the IUPHAR/BPS Guide to PHARMACOLOGY (Harding *et al.*, 2018), and are permanently archived in the Concise Guide to PHARMACOLOGY 2017/18 (Alexander *et al.*, 2017).

Cell Culture

HeLa ovarian carcinoma cells, Lewis lung carcinoma cells and B16F10 melanoma cells were purchased from ATCC and grown in DMEM supplemented with 10% heat-inactivated fetal bovine serum (FBS) and 1% penicillin/streptomycin (all from Invitrogen). Cells were tested for mycoplasma contamination every 1 month, and only mycoplasma-negative cells were used. Short tandem repeat (STR) DNA fingerprinting analysis was performed in 2016 for authentication of these cells.

Tumor formation and drug treatment

Tumor xenograft experiments were performed in 8- to 10-week-old mice challenged *s.c.* with 6×10^5 Lewis tumor cells or 2×10^5 B16F10 melanoma cells. Mice were randomly divided into 5 groups and injected *i.p.* daily with vehicle alone, LW106 at doses of 20 mg/kg, 40 mg/kg and 80 mg/kg or epacadostat at 80 mg/kg at day 6 following initial tumor cell engraftment until termination of the experiment. All compounds were dissolved freshly in sodium citrate buffer prior to each experiment. Tumor volume was measured every 2 days at day 3 post tumor inoculation using the formula $V = \pi \times \text{length} \times \text{width}^2/6$. Tumors were harvested, weighted and subjected to further use.

FACS analysis

For T cell assay, xenografted tumors were dissected, minced into small pieces and digested for 45 min at 37 °C in 1X HBSS buffer containing 2% FBS, 1 mg/ml

collagenase I (Sigma-Aldrich) and 0.5 mg/ml dispase (Invitrogen), followed by further digestion in 10 μg/ml DNase (Invitrogen) for 45 min, and 0.64% ammonium chloride (STEMCELL Technologies) for 5 min at 37 °C; Spleens from tumor-bearing mice were dissected into pieces and dissociated mechanically in D-Hank's buffer (Invitrogen) for 10 min on ice. Cells were filtered through a 70-μm cell strainer (BD Biosciences), resuspended in 1X HBSS buffer containing 2% FBS and subjected to a gradient centrifugation in Ficoll-Pague (Sigma-Aldrich). Purified lymphocytes were stained using a fixation and permeabilization kit (eBioscience) and analyzed by FACS analysis to detect expression of CD45, CD4, CD8, Foxp3 (all from Biolegend) and Ki67 (Cell Signaling). For CSC assay, xenografted tumors were dissected into pieces and dissociated enzymatically as described above. Cells were incubated with an antibody cocktail containing CD31, CD45 and Ter119 (STEMCELL Technologies), a secondary biotin-labelled antibody cocktail (STEMCELL Technologies) and magnetic beads (15 min each). The unbound cells (LIN^-) were collected and labelled with APC-CD44 or PE-CD144 (both from BD Biosciences) for 30 min at 4 °C, followed by DAPI staining for 5 min at 4 °C. Cells were washed extensively and subjected to ALDH activity assay using a kit from STEMCELL Technologies according to the manufacturer's instructions. The labelled cells were subjected to FACS analysis to detect ALDH activity and the expression of CD133 and CD44.

Lymphocyte and DC co-culture

Lymphocyte and DC co-culture were performed as described previously with slight modification (Liu *et al.*, 2010). PBMCs from healthy volunteers were subjected to centrifugal elutriation to obtain monocytes and lymphocytes. The purified monocytes were treated with 10 ng/ml human recombinant interleukin 4 (hIL-4; R & D Systems) and 40 ng/ml human recombinant granulocyte macrophage colony stimulating factors (hGM-CSF; R & D Systems) for 5 days, and the floating and loosely attached cells (*i.e.* $IDO1^-$ immature DCs) were harvested. $IDO1^+$ mature DCs were obtained by treating immature DCs with 50 ng/ml human recombinant interferon γ (hIFN-γ; Peprotech) and 1 μg/ml lipopolysaccharide (LPS; Sigma-Aldrich) for additional 2 days. $IDO1^+$ mature DCs or $IDO1^-$ immature DCs were co-cultured with purified lymphocytes in the presence of vehicle, LW106 or epacadostat for 2 days. Cells were harvested, stained with anti-CD8 antibody (Biolegend) and subjected to FACS analysis.

Tumorsphere assay

FACS-sorted single cells were plated in ultralow-attachment plates (2 X 10^4 cells/well; Corning) with serum-free DMEM/F12 medium (Invitrogen), supplemented with B27 (Invitrogen), 20 ng/ml EGF, 20 ng/ml bFGF (R & D Systems), and 4 mg/ml heparin (Sigma). Tumorspheres were counted 7 days after plating.

Tryptophan/kynurenine measurement

Tryptophan/kynurenine measurement were performed as described previously with slight modification (Liu *et al.*, 2010). To measure IDO1 enzyme activity *in vitro*, HeLa cells were stimulated with 50 ng/ml human recombinant IFN-γ for 48 h, and conditioned medium were collected, centrifuged to remove cell debris and stored at -20 °C for further use. To measure IDO1 enzyme activity *in vivo*, blood and Tumors from vehicle- or drug-treated mice were collected and stored at -20 °C for further use. Tumors were homogenized in 3 volumes of normal saline with 0.1% formic acid. Following protein-precipitation extraction with methanol, supernatants of conditioned medium, plasmas and tumor homogenates were collected and 20 μl of the supernatants were subjected to LC/MS/MS analysis. Aqueous standards were prepared for adjustment of endogenous tryptophan and kynurenine levels.

Histological and immunohistochemical analyses

For histology, tissues were fixed in 4% paraformaldehyde (PFA), embedded in paraffin and sectioned, followed by hematoxylin and eosin (H&E) staining. For immunohistochemical assay, paraffin-embedded sectioned were deparaffined, rehydrated and subjected to antigen heat retrieval with citric buffer, pH 6.0 (Vector Laboratories). The sections were treated with 0.5% H_2O_2 (Sigma-Aldrich) for 10 min at room temperature and further incubated in blocking buffer (5% goat serum in PBS) supplemented with primary antibodies against cleaved caspase 3 (Cell Signaling), Ki67 (Abcam) and p-Histone H3 (Cell Signaling) overnight at 4 °C, followed by incubation with biotinylated goat anti-rabbit secondary antibody (Vector Laboratories) at room temperature for 1 h. Standard ABC kit and DAB (Vector Laboratories) were used for the detection of HRP activity. Sections were counterstained with hematoxylin, dehydrated and mounted. In some experiments, sections were incubated in blocking buffer (5% goat serum in PBS) containing primary antibodies against CD31, α-SMA (both from Abcam), K14 (Biolegend) and CD8 (Biolegend) overnight at 4 °C, followed by incubation

with goat anti-rat Alexa 488, goat anti-rabbit Alexa 488 and goat anti-rabbit Alexa 594 secondary antibodies (all from Invitrogen) for 1 h at room temperature. Sections were stained with DAPI for 5-10 min at room temperature and mounted for confocal microscopy.

Immunoblotting assay

Cells were harvested and lysed in RIPA buffer (Thermo Scientific) containing proteinase inhibitor cocktail (Thermo Scientific) on ice for 20 min, followed by centrifugation for 20 min at 4°C, 14,000 *g*. The supernatants were collected and subjected to immunoblotting assay using anti-IDO1 antibody (Merck).

Cell survival assay

Tumor cells were seeded in 12-well culture plates and treated with vehicle or indicated compounds at different concentrations for 2 days. Cells were harvested, resuspended in trypan blue staining buffer (containing 0.04% trypan blue, Thermo Fisher) and cultured for 3 min at room temperature. Live cells (*i.e.* trypan blue exclusive cells) were instantly counted under light microscope, and survival rates of cells were calculated.

Kaplan-Meier survival analysis

Overall survival (OS), post-progression survival (PPS) and distant-metastasis-free survival (DMFS) rates were assessed in lung cancer patients (with indicated subtypes; Gyorffy *et al.*, 2010), ovarian cancer patients (Gyorffy *et al.*, 2012), breast cancer patients (Gyorffy *et al.*, 2013) and gastric cancer patients (Szasz *et al.*, 2016). The patients were divided as 'high' and 'low' groups by median *IDO1* expression. All other parameters were left as default settings.

Statistical analysis

All results wherever necessary were subjected to statistical analysis. Data are presented as mean ± S.E.M. Statistical analysis was performed as described in each corresponding figure legend. Sample sizes are shown in each corresponding figure legend. $P < 0.05$ is considered significant.

Results

Tumor cell-derived *IDO1* expression level does not correlate with cancer patient survival

To date, it is still controversial whether tumor cell-derived *IDO1* expression level

correlates with cancer patient survival (Holmgaard *et al.*, 2013). Using a Kaplan-Meier survival analysis (http://kmplot.com/analysis/), we failed to observe a statistically significant relationship between overall survival (OS), post-progression survival (PPS), and distant-metastasis-free survival (DMFS) rates and tumor cell-derived *IDO1* expression level in patients with various types of cancers such as lung, ovarian, breast or gastric cancer (Fig. 1A-H; Suppl. Fig. 2A-D). These data suggest that targeting IDO1 as a therapeutic strategy might be applicable to IDO1-expressing host-derived cells but not tumor cells.

LW106 inhibited IDO1 enzyme activity but did not affect tumor cell proliferation *in vitro*

To determine the *in vitro* inhibitory effect of LW106 on IDO1 enzyme activity, HeLa ovarian carcinoma cells were stimulated with IFN-γ and applied to an enzyme activity assay. It has been reported that expression level of IDO1 but not IDO2 or TDO was dramatically increased in the stimulated cells (Liu *et al.*, 2010). We observed that LW106 inhibited IDO1 enzyme activity with an IC_{50} value of 1.57 μM while did not affect IDO1 protein expression level in the stimulated cells (Suppl. Fig. 3A, B). Moreover, LW106 at doses ranging from 12.5 to 200 μM did not affect proliferation of three types of tumor cells with different expression levels of IDO1 (Suppl. Fig. 3C-E). It has been reported that $IDO1^+$ DCs can inhibit T-cell proliferation/survival, which is believed to be responsible for IDO1-mediated tumor escape (Mellor *et al.*, 2003). To examine whether LW106 could reverse IDO1-mediated T-cell suppression, $IDO1^+$ mature DCs or $IDO1^-$ immature DCs were co-cultured with purified lymphocytes in the presence of vehicle, LW106 or epacadostat. Co-cultured cells were harvested, stained with anti-CD8 antibody and subjected to FACS analysis. We found that IDO1 induction strongly suppressed $CD8^+$ T-cell proliferation/survival in the co-culture system, and the suppression could be effectively reversed by LW106 and epacadostat (Suppl. Fig. 4A, B).

LW106 dose-dependently inhibited outgrowth of IDO1-expressing tumor cells inoculated in immunocompetent C57BL6 mice but not athymic nude mice or *Ido1*$^{-/-}$ mice

To further determine the inhibitory effect of LW106 on outgrowth of tumor cells *in vivo*, immunocompetent C57BL6 mice were challenged with IDO1-expressing Lewis lung

carcinoma cells and treated with various doses of LW106 or epacadostat, an existing potent small molecule inhibitor of IDO1 that is currently in clinical trial for cancer treatment. We observed that LW106 dose-dependently inhibited tumor growth, reducing tumor weights by 30%, 54% and 68% at 20 mg/kg, 40 mg/kg and 80 mg/kg, respectively (Fig. 2A). Importantly, we failed to observe pathological changes in vital organs (*e.g.* heart, liver, lung and kidney) of mice that received LW106 treatment at 80 mg/kg (Suppl. Fig. 3A). Meanwhile, epacadostat treatment at 80 mg/kg reduced tumor weight by 51%, displaying a weaker antitumor efficacy as compared with LW106 (Fig. 2A). Similarly, a significant reduction in tumor volumes was observed in LW106-treated mice relative to vehicle-treated mice (Fig. 2B). A marked reduction in kynurenine/tryptophan ratio was also detected in plasmas and xenografts of LW106-treated mice (Fig. 2C). However, it should be noted that tryptophan depletion and GCN2 kinase activation may also play important roles in IDO1-mediated tumor immune escape (Mun *et al.*, 2005; Eleftheriadis *et al.*, 2014). Of note, both LW106- and epacadostat-treated mice displayed markedly increased survival compared with vehicle-treated mice (Fig. 2D). It has been documented that IDO1 enzyme inhibitors require intact T-cell function to suppress tumor growth in mice (Liu *et al.*, 2010). To evaluate the importance of T-cell-dependent immunity to the antitumor effect of LW106, athymic nude mice that are deficient in mature T cells were challenged with Lewis tumor cells and tumor outgrowth were monitored. In the context of these mice, LW106 treatment at 80 mg/kg had no distinguished effect on tumor outgrowth, suggesting that LW106 exerts its antitumor effect in a T-cell-dependent manner (Fig. 2E). We further applied *Ido1*$^{-/-}$ (*Ido1* knockout) mouse model to determine whether IDO1 blockade in the inoculated tumor cells or the host-derived cells is directly relevant to the mechanism of antitumor effect of LW106. Interestingly, we found that LW106 treatment at 80 mg/kg failed to suppress tumor outgrowth in Ido1$^{-/-}$ mice that were inoculated with IDO1-expressing Lewis tumors, suggesting that LW106 inhibited tumor outgrowth via blocking activity of IDO1 expressed by the host-derived cells but not the inoculated tumor cells (Fig. 2F).

LW106 dose-dependently inhibited outgrowth of IDO1-nonexpressing tumor cells inoculated in C57BL6 mice but not athymic nude mice or Ido1$^{-/-}$ mice

We extended our studies to further evaluate LW106 treatment in another widely used B16F10 melanoma tumor model (IDO1 is undetectable in B16F10 cells). Again, we

observed that tumor weights were reduced by 29%, 52% and 65% in mice treated with LW106 at 20 mg/kg, 40 mg/kg and 80 mg/kg, respectively (Fig. 3A). We did not observe pathological changes in vital organs (*e.g.* heart, liver, lung and kidney) of mice that received LW106 treatment at 80 mg/kg (Suppl. Fig. 5A, B). Epacadostat displayed a weaker antitumor efficacy than LW106, with a 50% reduction in tumor weight when administrated at 80 mg/kg (Fig. 3A). Additionally, a substantial decrease in tumor volumes was observed in LW106-treated mice relative to vehicle-treated mice (Fig. 3B). LW106 treatment at 80 mg/kg did not suppress outgrowth of B16F10 tumors that were inoculated in athymic nude mice or Ido1$^{-/-}$ mice (Fig. 3C, D), further support the notion that T-cell immunity and IDO1 targeting in the host-derived cells are essential for antitumor efficacy of LW106.

LW106 treatment enhanced infiltration and accumulation of T cells in xenografted tumors

Given that T-cell-dependent immunity is essential for tumor-suppressive activity of LW106, we sought to study the effector T cell and regulatory T cell compartments within the Lewis and B16F10 tumors following LW106 treatment. For this purpose, tumors were harvested 18 days after implantation, and tumor-infiltrating lymphocytes were isolated and subjected to FACS analysis. We observed a significantly increased number of tumor-infiltrating CD8 effector T cells (CD8$^+$CD45$^+$) in mice treated with LW106 as compared with vehicle-treated mice (Fig. 4A; Suppl. Fig. 6A). LW106 treatment also increased infiltration of proliferative CD8 effector T cells within the xenografted tumors, as measured by expression of Ki67, a widely used cell proliferating marker (Fig. 4B). By contrast, infiltration of regulatory T cells (CD4$^+$Foxp3$^+$CD45$^+$) was robustly reduced in LW106-treated mice relative to vehicle-treated mice (Fig. 4C). A dramatic decrease in the percentage of proliferative regulatory T cells was observed within xenografted tumors of LW106-treated mice (Fig. 4D; Suppl. Fig. 6B). Intratumoral ratios of CD4 effector T cells (CD4$^+$Foxp3$^-$CD45$^+$) to regulatory T cells were markedly elevated in LW106-treated mice as compared with vehicle-treated mice (Fig. 4E; Suppl. Fig. 6C). Additionally, immunofluorescence analysis further revealed a robustly increased infiltration of proliferative CD8 effector T cells (Ki67$^+$CD8$^+$) within xenografted tumors of LW106-treated mice (Fig. 4F; Suppl. Fig. 6D).

LW106 treatment enhanced accumulation of splenic T cells in Lewis

tumor-bearing mice

Because spleen serves as an important reservoir for lymphocytes that can be recruited to the tumor sites and directly involve in antitumor immunity, we therefore sought to study the effector T cell and regulatory T cell compartments in the spleens of tumor-bearing mice. We observed markedly enlarged spleens in mice that received LW106 treatment as compared with epacadostat- or vehicle-treated mice (Fig. 5A, B). Importantly, H.E. staining of spleens from LW106-treated mice revealed no distinguished pathological changes (Fig. 5C). Flow cytometry analysis of splenocytes revealed a higher percentage of CD8 effector T cells in the spleens of LW106-treated mice as compared to vehicle-treated mice (Fig. 5D). Furthermore, LW106 treatment significantly increased the percentage of proliferative CD8 and CD4 effector T cells in tandem with a marked reduction in the percentage of proliferative regulatory T cells in the spleens (Fig. 5E-G). Taken together, these results suggest that LW106 treatment increased the number of splenic effector T cells that can be recruited to the tumor sites and function there.

LW106 treatment resulted in impaired proliferation and survival of tumor cells in tandem with reduced recruitment of non-hemopoietic stromal cells and deposition of extracellular matrix in the TME

The data above had shown that tumor outgrowth was significantly inhibited in LW106-treated mice. We next sought to determine whether LW106 treatment could affect the proliferation and survival of tumor cells within Lewis and B16F10 tumors. For this purpose, we performed immunohistochemical staining of Ki67 (a proliferative cell marker), phospho-Histone H3 (a mitotic cell marker) and cleaved caspase 3 (an apoptotic cell marker) in the xenografted tumors. We found that the percentages of proliferative and mitotic cells were markedly decreased in tumors of LW106-treated mice relative to vehicle-treated mice (Fig. 6A; Suppl. Fig. 7A). By contrast, the percentage of apoptotic cells was significantly increased in tumors of LW106-treated mice (Fig. 6A; Suppl. Fig. 7A). A reduced number of cytokeratin-14 (K14)-positive tumor cells (*i.e.* invasive tumor cells) was also observed in tumors of LW106-treated mice (Fig. 6B). These data suggest that LW106 treatment decreases the proliferation, survival and invasiveness of tumor cells, thus suppressing tumor outgrowth.

The relationship between the stroma and tumor-infiltrating lymphocytes remains largely

uncharacterized (Turley *et al.*, 2015). Emerging evidences have suggested that the stromal compartments (*e.g.* cancer-associated fibroblasts, endothelial cells as well as extracellular matrix) can shape antitumor immunity and responsiveness to immunotherapy (Turley *et al.*, 2015). We therefore sought to determine whether LW106 treatment could affect the recruitment of non-hematopoietic stromal cells and the deposition of stroma-derived extracellular matrix in the TME, which may contribute to its antitumor effect. Immunohistochemical assay showed that type I collagen expression level was significantly decreased in tumors of LW106-treated mice, indicating a reduced extracellular matrix deposition in the tumors following LW106 treatment (Fig. 6B; Suppl. Fig. 7B). We further observed that the percentages of CD31-positive cells (*i.e.* endothelial cells) and α-smooth muscle actin (α-SMA)-positive cells (*i.e.* cancer-associated fibroblasts) were substantially reduced in tumors of LW106-treated mice as compared with vehicle-treated mice (Fig. 6B; Suppl. Fig. 7B). These data illustrated that targeting IDO1 in host-derived cells by LW106 inhibited recruitment of non-hematopoietic stromal cells and deposition of extracellular matrix, which could generate a tumor-suppressive microenvironment within the tumors and thus suppress tumor outgrowth.

LW106 treatment inhibited enrichment of cancer stem cells in xenografted tumors

Cancer stem cells (CSCs), a population tumor cells that possess the defining features of clonogenicity and self-renewal, are proposed to have a critical role in tumor progression, metastasis and drug resistance (Ni *et al.*, 2016; Codony-Servat *et al.*, 2016; Hardavella *et al.*, 2016). CSCs in human lung tumors were identified using a list of markers such as CD133, CD44 and ALDH1 (Codony-Servat *et al.*, 2016; Hardavella *et al.*, 2016). To test whether these markers could also be used for identification of CSCs in Lewis xenografted tumors, we sorted tumor cells using FACS with these markers and performed *in vitro* tumorsphere assays. Although we could not detect CD133 expression in the xenografted tumors (data not shown), we indeed observed that $ALDH^+$ or $CD44^+ALDH^+$ cells possessed the potentials to form tumorsphere (Fig. 7A). These results suggest that both CD44 and ALDH1 can be used as markers for identification of CSCs in Lewis xenografted tumors. We further found that xenografted tumors of LW106-treated mice displayed markedly reduced numbers of $CD44^+$, $ALDH^+$ or $CD44^+ALDH^+$ cells as compared with vehicle-treated mice (Fig. 7B), which may be

attributed to the regression of tumors observed in LW106-treated mice (Fig. 2A).

Discussion

Inhibition of IDO1 is a very promising area of cancer immunotherapy. Three small-molecule inhibitors of IDO1, 1-methyl-tryptophan (1-MT), NLG919 and epacadostat, are currently in clinical trials for treatment of various types of cancer including non-small cell lung cancer (NSCLC), ovarian cancer and melanoma (Cady *et al.*, 1991; Jackson *et al.*, 2013; Liu *et al.*, 2010). These compounds possess potential immunomodulating and antineoplastic activities by inhibiting IDO1 enzyme activity in the tumor cells and host-derived immune cells such as DCs and macrophages (Cady *et al.*, 1991; Jackson *et al.*, 2013; Liu *et al.*, 2010). In the present study, we have discovered LW106 as a structurally novel, selective and potent small-molecule inhibitor of IDO1. In comparison with epacadostat, LW106 showed a weaker *in vitro* inhibition on IDO1 enzyme activity when assayed in IFN-γ-stimulated HeLa cells, but indeed displayed a stronger antitumor efficacy in mice bearing xenografted tumors. It is unlikely that the antitumor activity of LW106 is due to the "off-target" effect as the compound does not suppress tumor outgrowth in *Ido1*$^{-/-}$ mice. A possible explanation for the distinguished inhibition performed by LW106 *in vitro* versus *in vivo* is that LW106 might be metabolized into potential metabolite(s) *in vivo* that can inhibit IDO1 enzyme activity more efficiently than LW106 itself, and further work is required to identify and synthesize the potential metabolite(s) and evaluate their antitumor efficacy. Nevertheless, LW106 can be considered as a potent and selective inhibitor of IDO1 since treatment with the compound causes a strong tumor regression in IDO1-intact mice but fails to inhibit tumor outgrowth in IDO1-deficient mice.

Inhibition of IDO1 enzyme activity in tumor cells appears not to affect cell growth *in vitro* as tumor cells grow normally when treated with LW106 at a concentration of over 100-fold higher than EC50. The inhibitory effect of LW106 on tumor outgrowth *in vivo* is related to IDO1 expression by host-derived immune cells but not tumor cells since LW106 administrated *in vivo* display a comparable inhibitory effect on proliferation of IDO1-expressing xenografts versus IDO1-nonexpressing xenografts. In addition, Kaplan-Meier survival analysis reveals that the mRNA levels of IDO1 expressed by tumor cells do not correlate with the survivals in patients with various types of cancers

such as lung, ovarian, breast or gastric cancer. Hence, it is reasonable to propose that IDO1 expression by host-derived cells rather than tumor cells can be used as a predictive marker for response to therapy with LW106 as well as other selective inhibitors of IDO1 such as NLG919 (Jackson *et al.*, 2013) and epacadostat (Liu *et al.*, 2010) and that such immunotherapy can also be beneficial for patients with undetectable IDO1 expression in tumor cells.

Emerging evidence suggests that the stromal compartment in the TME may hinder antitumor immune response via actively interacting with the surrounding immune cells (Joyce *et al.*, 2009; Turley *et al.*, 2015). For instance, non-hematopoietic stromal cells such as cancer-associated fibroblasts (CAFs) and endothelial cells (ECs) express numerous surface and secreted molecules to directly suppress $CD4^+$ and $CD8^+$ effector T cells and activate suppressive myeloid cells and $CD4^+$ regulatory T cells (Joyce *et al.*, 2009; Buckanovich *et al.*, 2008; Castermans *et al.*, 2007; Feig *et al.*, 2013; Tan *et al.*, 2011). The stroma-derived extracellular matrix (ECM) in the TME may also suppress antitumor immune response by limiting T cell motility and localization (Joyce *et al.*, 2009; Caruana *et al.*, 2015; Provenzano *et al.*, 2012; Salmon *et al.*, 2012). Of note, immune cells including regulatory T cells, cancer-associated macrophages (CAMs; $F4/80^+$ cells) and suppressive myeloid cells also secret numerous molecules, to directly support activation and survival of stromal cells (Joyce *et al.*, 2009; Beatty *et al.*, 2011; Coussens *et al.*, 2013; Lu *et al.*, 2011; Turley *et al.*, 2015). In the current study, we have discovered that LW106 profoundly inhibits stromal cell recruitment and ECM deposition in the TME, which in turn causes an impaired crosstalk between stromal compartment and T cells, thus promoting T cell immune response to tumors. On the other hand, our data suggest that targeting IDO1 in host-derived cells by LW106 strongly suppresses infiltration of $CD4^+Foxp3^+$ regulatory T cells and $F4/80^+$ CAMs (data not shown), which consequently results in an impaired immune-stroma interaction, thus limiting recruitment, activation and survival of stromal cells in the TME. Further work is required to define the precise mechanisms by which LW106 inhibits recruitment, activation and survival of non-hematopoietic stromal cells in the TME. In addition to the immunomodulatory role, stromal compartment in the TME may also have a critical role in controlling cancer stem cell (CSC) expansion (Joyce *et al.*, 2009; Buckanovich *et al.*, 2008). Herein, we demonstrate that the expansion of CSCs is strongly suppressed in

tumors of LW106-treated mice, suggesting that the inhibitory effect of LW106 on tumor growth and chemoresistance can, at least in part, be attributed to reduced CSC enrichment in the TME.

In conclusion, the data presented here suggest that LW106 inhibits tumor growth by limiting stroma-immune crosstalk and CSC enrichment in the TME, and that LW106 can be further developed as a potential immunotherapeutic agent used in combination with immune checkpoint inhibitors and (or) chemotherapeutic drugs for cancer treatment.

Financial support: This work was supported by the National Natural Science Foundation of China (81572745, 91539115 and 81603134), the Jiangsu Provincial Natural Science Fund for Distinguished Young Scholar (BK20170029), the Jiangsu Provincial Natural Science Fund for Young Scholar (BK20160758), the Jiangsu Provincial Innovative Research Program, the fund from State Key Laboratory of Natural Medicines of China Pharmaceutical University (SKLNMZZJQ201604) and the fund from Collaborative Innovation Center for Gannan Oil-Tea Camellia Industrial Development (YP201608).

Author contributions: R.F. designed and performed experiments, analyzed data and wrote the paper. Y-W.Z. and H.-M.L. performed experiments and analyzed data. W.-C.L. and L.Z. performed experiments. Q.-L.G., S.J.W. and T.L. provided relevant advice. Z.-Y.L. provided compound. Z.-Q.W. oversaw the project, designed experiments, analyzed data and wrote the paper.

Conflict of interest: The authors declare no conflict of interest.

References

Alexander S PH, Fabbro D, Kelly E, Marrion N V, Peters J A , Faccenda E, et al. (2017). The Concise Guide to pharmacology: Enzymes. The concise guide to pharmacology 174: 272-359

Beatty GL, Chiorean EG, Fishman MP, Saboury B, Teitelbaum UR, Sun W, et al. (2011). CD40 agonists alter tumor stroma and show efficacy against pancreatic carcinoma in mice and humans. Science 331: 1612-1616.

Bhowmich NA, Neilson EG, Moses HL (2004). Stromal fibroblasts in cancer initiation and progression. Nature 432: 332-337.

Botting NP (1995) Chemistry and neurochemistry of kynurenine pathway of tryptophan metabolism. Chem Soc Rev 24: 401-412.

Brandacher G, Perathoner A, Ladurner R, Schneeberger S, Obrist P, Winkler C, et al. (2006). Prognostic value of indoleamine 2,3-dioxygenase expression in colorectal cancer: effect on tumor-infiltrating T cells. Clin Cancer Res 12: 1144-1151.

Buckanovich RJ, Facciabene A, Kim S, Benencia F, Sasaroli D, Balint K, et al. (2008). Endothelin B receptor mediates the endothelial barrier to T cell homing to tumors and disables immune therapy. Nat Med 14: 28-36.

Cady SG, Sono M (1991). 1-methyl-DL-tryptophan, β-(3-benzofurany)-DL-alanine, and β-[3-benzo(b)thienyl]-DL-alanine are competitive inhibitors for indoleamine 2,3-dioxygenase. Arch Biochem Biophys 291: 326-333.

Caruana I, Savoldo B, Hoyos V, Weber G, Liu H, Kim ES, et al. (2015). Heparanase promotes tumor infiltration and antitumor activity of CAR-redirected T lymphocytes. Nat Med 21: 524-529.

Castermans K, Griffioen AW (2007). Tumor blood vessels, a difficult hurdle for infiltrating leukocytes. Biochem Biophys Acta 1776: 160-174.

Codony-Servat J, Verlicchi A, Rosell R (2016). Cancer stem cells in small cell lung cancer. Transl Lung Cancer Res 5: 16-25.

Coussen LM, Werb Z (2002). Inflammation and cancer. Nature 420: 860-867.

Coussens LM, Zitvogel L, Palucka AK (2013). Neutralizing tumor promising chronic inflammation: a magic bullet? Science 339: 286-291.

Eleftheriadis T, Pissas G, Antoniadi G, Spanoulis A, Liakopoulos V, Stefanidis L (2014). Indoleamine 2,3-dioxygenase increases p53 levels in alloreactive human T cells, and both indoleamine 2,3-dioxygenase and p53 suppress glucose uptake, glycolysis and proliferation. Int Immunol 26: 673-684.

Fallarino F, Grohmann U, Vacca C, Bianchi R, Orabona C, Spreca A, et al. (2002). T cell apoptosis by tryptophan catabolism. Cell Death Differ 9: 1069-1077.

Feig C, Jones JO, Kraman M, Wells RJ, Deonarine A, Chan DS, et al. (2013). Targeting CXCL12 from FAP-expressing carcinoma-associated fibroblasts synergizes with anti-PD-L1 immunotherapy in pancreatic cancer. Proc Natl Acad Sci U S A 110:

20212-20217.

Frumento G, Rotondo R, Tonetti M, Damonte G, Benatti U, Ferrara GB (2002). Tryptophan-derived catabolites are responsible for inhibition of T and natural killer cell proliferation induced by indoleamine 2,3-dioxygenase. J Exp Med 196: 459-468.

Gyorffy B, Lanczky A, Eklund AC, Denkert C, Budczies J, Li Q, et al. (2010). An online survival analysis tool to rapidly assess the effect of 22,277 genes on breast cancer prognosis using microarray data of 1809 patients. Breast Cancer Res Treat 123: 725-31.

Gyorffy B, Lanczky A, Szallasi Z (2012). Implementing an online tool for genome-wide validation of survival-associated biomarkers in ovarian-cancer using microarray data of 1287 patients. Endocr-Relat Cancer 19: 197-208.

Gyorffy B, Surowiak P, Budczies J, Lanczky A (2013). Online survival analysis software to assess the prognostic value of biomarkers using transcriptomic data in non-small-cell lung cancer. PLoS ONE 8: e82241.

Hanahan D, Coussens LM (2012). Accessories to the crime: functions of cells recruited to the tumor microenvironment. Cancer Cell 21: 309-322.

Hardavella G, George R, Sethi T (2016). Lung cancer stem cells-characteristics, phenotype. Transl Lung Cancer Res 5: 272-279.

Harding SD, Sharman JL, Faccenda E, Southan C, Pawson AJ, Ireland S et al. (2018). The IUPHAR/BPS Guide to PHARMACOLOGY in 2018: updates and expansion to encompass the new guide to IMMUNOPHARMACOLOGY. Nucl Acids Res 46: 1091-1106.

Hanahan D, Weinberg RA (2011). Hallmarks of cancer: the next generation. Cell 144: 646-674.

Holmgaard RB, Zamarin D, Munn DH, Wolchok JD, Allison JP (2013). Indoleamine 2,3-dioxygenase is a critical resistance mechanism in antitumor T cell immunotherapy targeting CTLA-4. J Exp Med 210: 1389-1402.

Ino K, Yamamoto E, Shibata K, Kajiyama H, Yoshida N, Terauchi M, et al. (2008). Inverse correlation between tumoral indoleamine 2,3-dioxygenase expression and tumor-infiltrating lymphocytes in endometrial cancer: its association with disease progression and survival. Clin Cancer Res 14: 2310-2317.

Jackson E, Dees EC, Kauh JS, Harvey RD, Neuger A, Lush R, et al. (2013). A phase I

study of indoximod in combination with docetaxel in metastatic solid tumors. 2013 ASCO Annual Meeting. J Clin Oncol 31(suppl; abstr 3026).

Johansson M, Denardo DG, Coussens LM (2008). Polarized immune responses differentially regulate cancer development. Immunol Rev 222: 145-154.

Joyce JA, Pollard JW (2009). Microenvironmental regulation of metastasis. Nat Rev Cancer 9: 239-252.

Liu X, Shin N, Koblish HK, Yang G, Wang Q, Wang K, et al. (2010). Selective inhibition of IDO1 effectively regulates mediators of antitumor immunity. Blood 115: 3520-3530.

Lu P, Takai K, Weaver VM, Werb Z (2011). Extracellular matrix degradation and remodeling in development and disease. Cold Spring Harb Perspect Biol 3: a005058.

Mellor AL, Baban B, Chandler P, Marshall B, Jhaver K, Hansen A, et al. (2003). Induced indoleamine 2,3 dioxygenase expression in dendritic cell subsets suppresses T cell clonal expansion. J Immunol 171: 1652-1655.

Munn DH, Mellor AL (2004). IDO and tolerance to tumors. Trans Mol Med 10: 15-18.

Munn DH, Mellor AL (2007). Indoleamine 2,3-dioxygenase and tumor-induced tolerance. J Clin Invest 117: 1147-1154.

Munn DH, Shafizadeh E, Attwood JT, Bondarev I, Pashine A, Mellor AL (1999). Inhibition of T cell proliferation by macrophage tryptophan catabolism. J Exp Med 189: 1363-1372.

Munn DH, Sharma MD, Baban B, Harding HP, Zhang Y, Ron D, et al. (2005). GCN2 kinase in T cells mediates proliferative arrest and anergy induction in response to indoleamine 2,3-dioxygenase. Immunity 22: 633-642.

Munn DH, Sharma MD, Lee JR, Jhaver KG, Johnson TS, Keskin DB, et al. (2002). Potential regulatory function of human dendritic cells expressing indoleamine 2,3-dioxygenase. Science 297: 1867-1870.

Ni T, Li X-Y, Lu N, An T, Liu Z-P, Fu R, et al. (2016). Snail1-dependent p53 repression regulates expansion and activity of Tumor-initiating cells in breast cancer. Nat Cell Biol 18: 1221-1232.

Pan K, Wang H, Chen MS, Zhang HK, Weng DS, Zhou J, et al. (2008). Expression and prognosis role of indoleamine 2,3-dioxygenase in hepatocellular carcinoma. J Cancer Res Clin Oncol 134: 1247-1253.

Polak ME, Borthwich NJ, Gabriel FG, Johnson P, Higgins B, Hurren J, et al. (2007).

Mechanisms of local immunosuppression in cutaneous melanoma. Br J Cancer 96: 1879-1887.

Prendergast GC (2008). Immune escape as a fundamental trait of cancer: focus on IDO. Oncogene 27: 3889-3900.

Provenzano PP, Cuevas C, Chang AE, Goel VK, Von Hoff DD, Hingorani SR (2012). Enzymatic targeting of the stroma ablates physical barriers to treatment of pancreatic ductal adenocarcinoma. Cancer Cell 21: 418-429.

Salmon H, Franciszkiewicz K, Damotte D, Dieu-Nosjean MC, Validire P, Trautmann A, et al. (2012). Matrix architecture defines the preferential localization and migration of T cells into the stroma of human lung Tumors. J Clin Invest 122: 899-910.

Sono M, Hayaishi O (1980). The reaction mechanism of indoleamine 2,3-dioxygenase. Biochem Rev 50: 173-181.

Sono M, Roach MP, Coulter ED, Dawson JH (1996). Heme-containing oxygenases. Chem Rev 96: 2841-2888.

Szasz AM, Lanczky A, Nagy A, Forster S, Hark K, Green JE, et al. (2016). Cross-validation of survival associated biomarkers in gastric cancer using transcriptomic data of 1,065 patients. Oncotarget 7: 49322-49333.

Tan W, Zhang W, Strasner A, Grivennikov S, Cheng JQ, Hoffman RM, et al. (2011). Tumor-infiltrating regulatory T cells stimulate mammary cancer metastasis through RANKL-RANK signaling. Nature 470: 548-553.

Turley SJ, Cremasco V, Astarita JL (2015). Immunological hallmarks of stromal cells in the tumor microenvironment. Nat Rev Immunol 15: 669-682.

Figure legends

Figure 1. Tumor cell-derived *IDO1* expression level does not correlate with cancer patient survival. Kaplan-Meier survival analysis of the relationship between survival rates and tumor cell-derived *IDO1* expression level in patients with various types of cancers. (**A, B**) Relationship between overall survival (OS; **A**) and post-progression survival (PPS; **B**) rates and *IDO1* expression level in lung cancer patients. (**C, D**) Relationship between OS (**C**) and PPS (**D**) rates and *IDO1* expression level in ovarian cancer patients. (**E-G**) Relationship between OS (**E**), PPS (**F**) and DMFS (**G**) rates and *IDO1* expression level in breast cancer patients. (**H**) Relationship between OS rate and

IDO1 expression level in gastric cancer patients. Differences between two survival curves are measured by Log-Rank Test. *n* represents the number of patients.

Figure 2. Lewis tumor outgrowth suppression by LW106 depends on T cells and IDO1 targeting. Mice were administrated *i.p.* daily with indicated compounds at day 6 following *s.c.* challenge with 6×10^5 Lewis tumor cells. (**A**) Tumor weights in immunocompetent mice (n = 6 mice, each). (**B**) Individual tumor growth in immunocompetent mice (n = 6 mice, each). (**C**) Ratio of tryptophan to kynurenine concentration in plasmas and xenografted tumors from immunocompetent mice (n = 6 mice, each). (**D**) Kaplan-Meier survival curves for tumor-bearing mice that were treated with vehicle, LW106 and epacadostat (n = 6 mice, each). (**E, F**) Individual tumor growth in BALB/c nude mice (**E**) and *Ido1*$^{-/-}$ mice (**F**) (n = 5 mice, each). Statistical significance was evaluated by two-way ANOVA test (A, B, C, E and F; * $P < 0.05$; ** $P < 0.01$; *** $P < 0.001$; $^{\#}$ $P < 0.05$) and Log-Rank Test (D; ** $P < 0.01$).

Figure 3. B16F10 melanoma outgrowth suppression by LW106 is dependent on T cells and IDO1 targeting. Mice were administrated *i.p.* daily with indicated compounds at day 6 following *s.c.* challenge with 2×10^5 B16F10 melanoma cells. (**A**) Tumor weights in immunocompetent mice (n = 6 mice, each). (**B**) Individual tumor growth in immunocompetent mice (n = 6 mice, each). (**C, D**) Individual tumor growth in BALB/c nude mice (**C**) and *Ido1*$^{-/-}$ mice (**D**) (n = 5 mice, each). Statistical significance was evaluated by two-way ANOVA test (* $P < 0.05$; ** $P < 0.01$; *** $P < 0.001$; $^{\#}$ $P < 0.05$).

Figure 4. LW106 treatment enhances infiltration and accumulation of T cells in xenografted tumors. Lewis tumors from vehicle-, LW106- and epacadostat-treated mice were harvested 18 days after tumor inoculation and subjected to FACS and immunofluorescent analyses. (**A**) Representative dot plots and percentage of $CD8^+$ effector T cells of total $CD45^+$ cells for vehicle-, LW106- and epacadostat-treated mice (n = 5 mice, each). (**B**) Representative dot plots and percentage of $CD8^+$ effector T cells expressing Ki67 for indicated mice as shown in *A*. (**C**) Percentage of $CD4^+Foxp3^+$ regulatory T cells of total $CD45^+$ cells for indicated mice as shown in *A*. (**D**) Percentage of $CD4^+Foxp3^+$ regulatory T cells expressing Ki67 for indicated mice as shown in *A*. (**E**) Ratio of $CD4^+Foxp3^-$ effector T cells to $CD4^+Foxp3^+$ regulatory T cells in tumors of indicated mice as shown in *A*. (**F**) Representative immunofluorescent images (*left panels*; images are representative of images from five mice) and percentage of $CD8^+$ T

cells expressing Ki67 for tumors of indicated mice (*right panel*; 1000 ~ 2000 cells were counted in 10 random fields of each slide). Arrow head denotes $Ki67^+CD8^+$ cells. Statistical significance was evaluated by two-way ANOVA test (* $P < 0.05$; ** $P < 0.01$; N.S., not significant).

Figure 5. LW106 treatment enhances accumulation of splenic T cells in Lewis tumor-bearing mice. Spleens from Lewis tumor-bearing mice that were treated with vehicle, LW106 and epacadostat were harvested and subjected to FACS and histological analyses. (**A**) Gross examination of spleens from tumor-bearing mice that were treated with indicated compounds (*n* = 6 mice, each). (**B**) Spleen weights in tumor-bearing mice as shown in *A*. (**C**) H.E. staining of spleens as shown in *A*. (**D**) Representative dot plots and percentage of $CD8^+$ effector T cells of total $CD45^+$ cells for spleens of tumor-bearing mice that were treated with indicated compounds (n = 6 mice in 3 pools, each). (**E**) Representative dot plots and percentage of $CD8^+$ effector T cells expressing Ki67 for spleens of tumor-bearing mice as shown in *D*. (**F, G**) Percentages of $CD4^+Foxp3^-$ effector T cells (**F**) and $CD4^+Foxp3^+$ regulatory T cells (**G**) expressing Ki67 for spleens of tumor-bearing mice as shown in *D*. Statistical significance was evaluated by two-way ANOVA test (* $P < 0.05$; ** $P < 0.01$; N.S., not significant).

Figure 6. LW106 treatment results in impaired proliferation and survival of Lewis tumor cells in tandem with reduced recruitment of tumor-associated stromal cells and deposition of extracellular matrix. Lewis xenografted tumors from vehicle-, LW106- and epacadostat-treated mice were harvested 18 days after tumor challenge and analyzed by immunohistochemistry. (**A**) Representative immunohistochemical images (*left panels*; images are representative of images from six mice) and percentages of Ki67-, phospho-histone H3- and cleaved caspase 3-positive cells for tumors of indicated mice (*right panels*; 1000 ~ 2000 cells were counted in 10 random fields of each slide). (**B**) Representative immunofluorescent images (*left panels*; images are representative of images from six mice), percentage of Ki67-positive cells (*1st row* at *right panels*; 1000 ~ 2000 cells were counted in 10 random fields of each slide) and relative fluorescent intensities of type I collagen, CD31 and α-SMA (*rest rows* at *right panels*; relative fluorescent intensities were calculated in 10 random fields of each slide) for tumors of indicated mice (*n* = 6 mice, each). Statistical significance was evaluated by two-way ANOVA test (* $P < 0.05$; ** $P < 0.01$; *** $P < 0.01$; $^{\#}$ $P < 0.05$; $^{\#\#}$ $P < 0.01$; N.S.,

not significant).

Figure 7. LW106 treatment inhibits cancer stem cell enrichment in Lewis tumors. Tumors from vehicle-, LW106- and epacadostat-treated mice were harvested 18 days after tumor challenge and subjected to FACS and tumorsphere assays. (**A**) Representative tumorsphere images (*left panels*; images are representative of images from six xenografted tumors in three pools) and number of tumorspheres formed by FACS-sorted $CD44^{-}ALDH^{-}$, $ALDH^{+}$ and $CD44^{+}ALDH^{+}$ Tumor cells of Lewis xenografts (*right panels*; n = 3 independent experiments). (**B**) Representative dot plots (*left panels*; plots are representative of plots from six mice in 3 pools) and percentages of $CD44^{+}$, $ALDH^{+}$ and $CD44^{+}ALDH^{+}$ cancer stem cells for tumors of indicated mice (*right panels*; n = 6 mice in 3 pools). Statistical significance was evaluated by two-way ANOVA test (* $P < 0.05$; ** $P < 0.01$; *** $P < 0.001$; $^{\#\#}$ $P < 0.01$).

Fig. 1

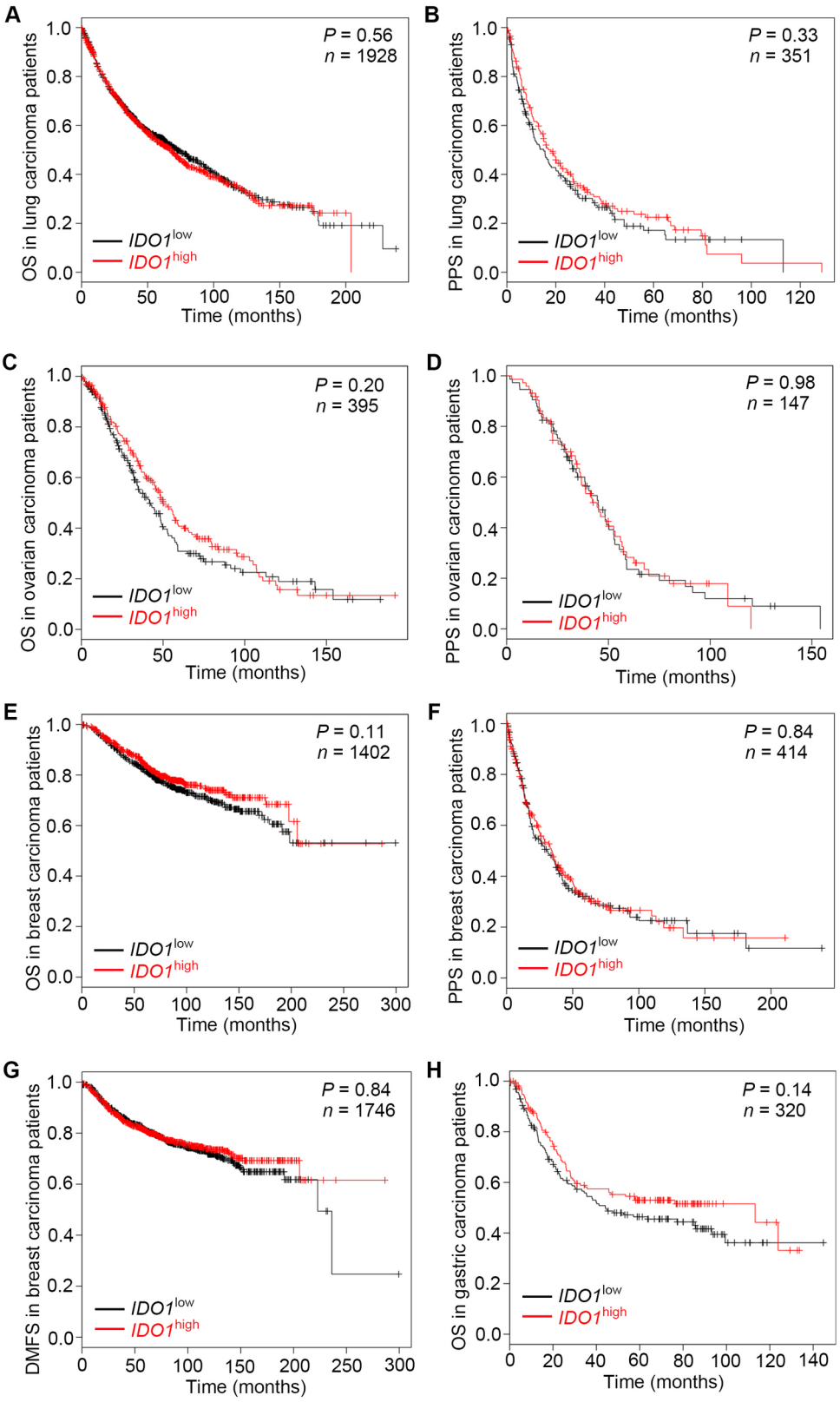

BPH_14351_F1.jpg

Fig. 2

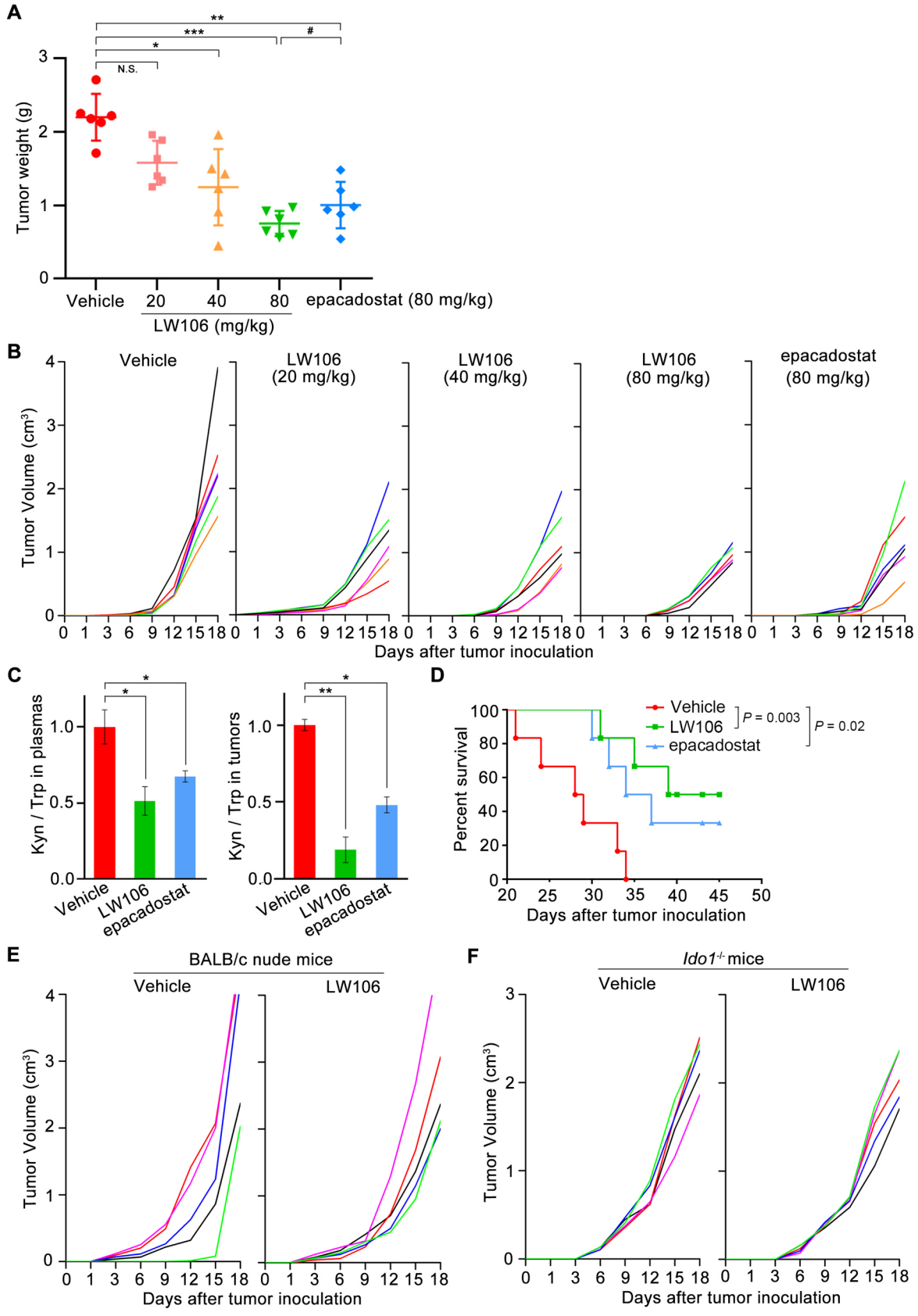

BPH_14351_F2.jpg

Fig. 3

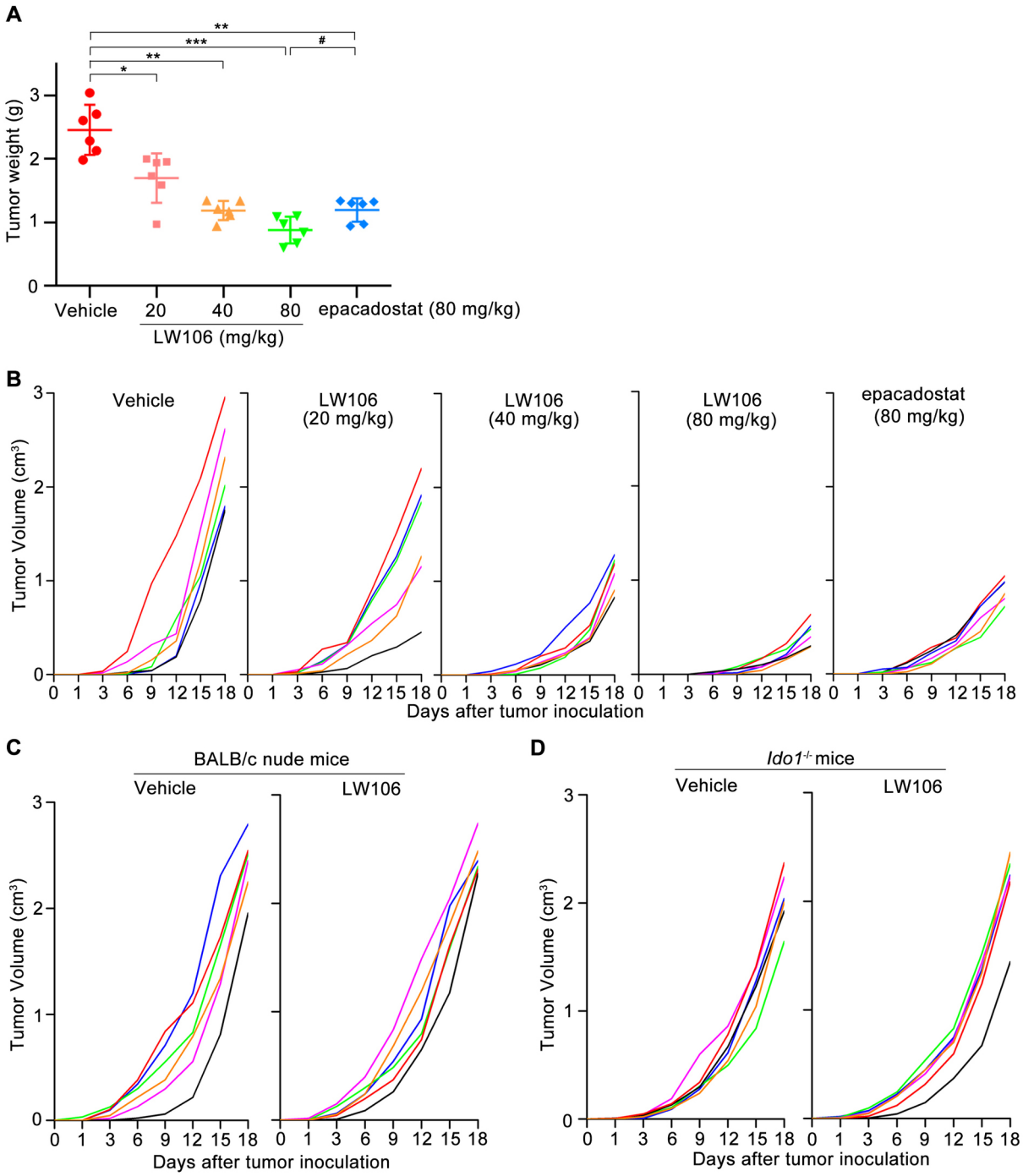

BPH_14351_F3.jpg

Fig. 4

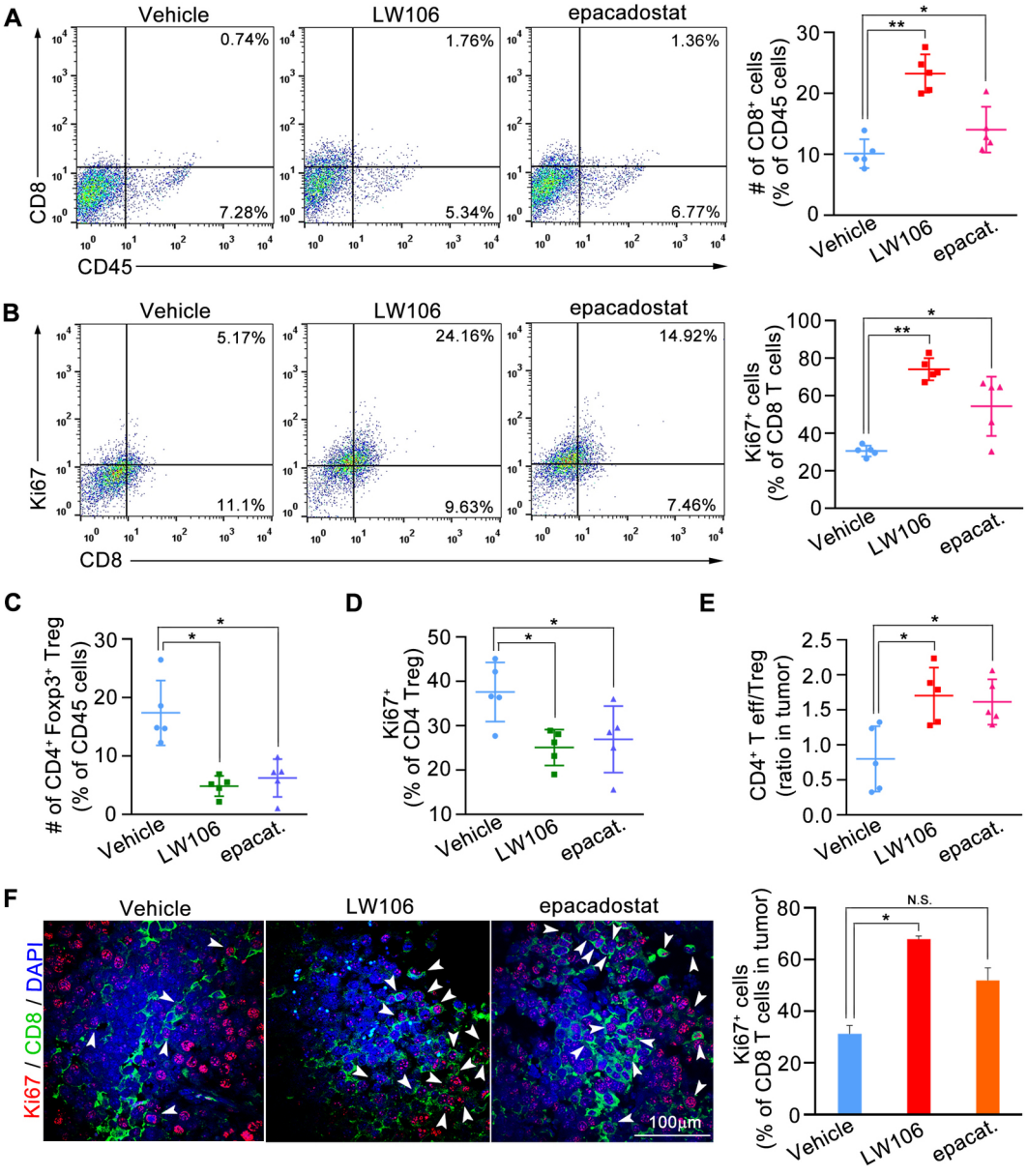

BPH_14351_F4.jpg

Fig. 5

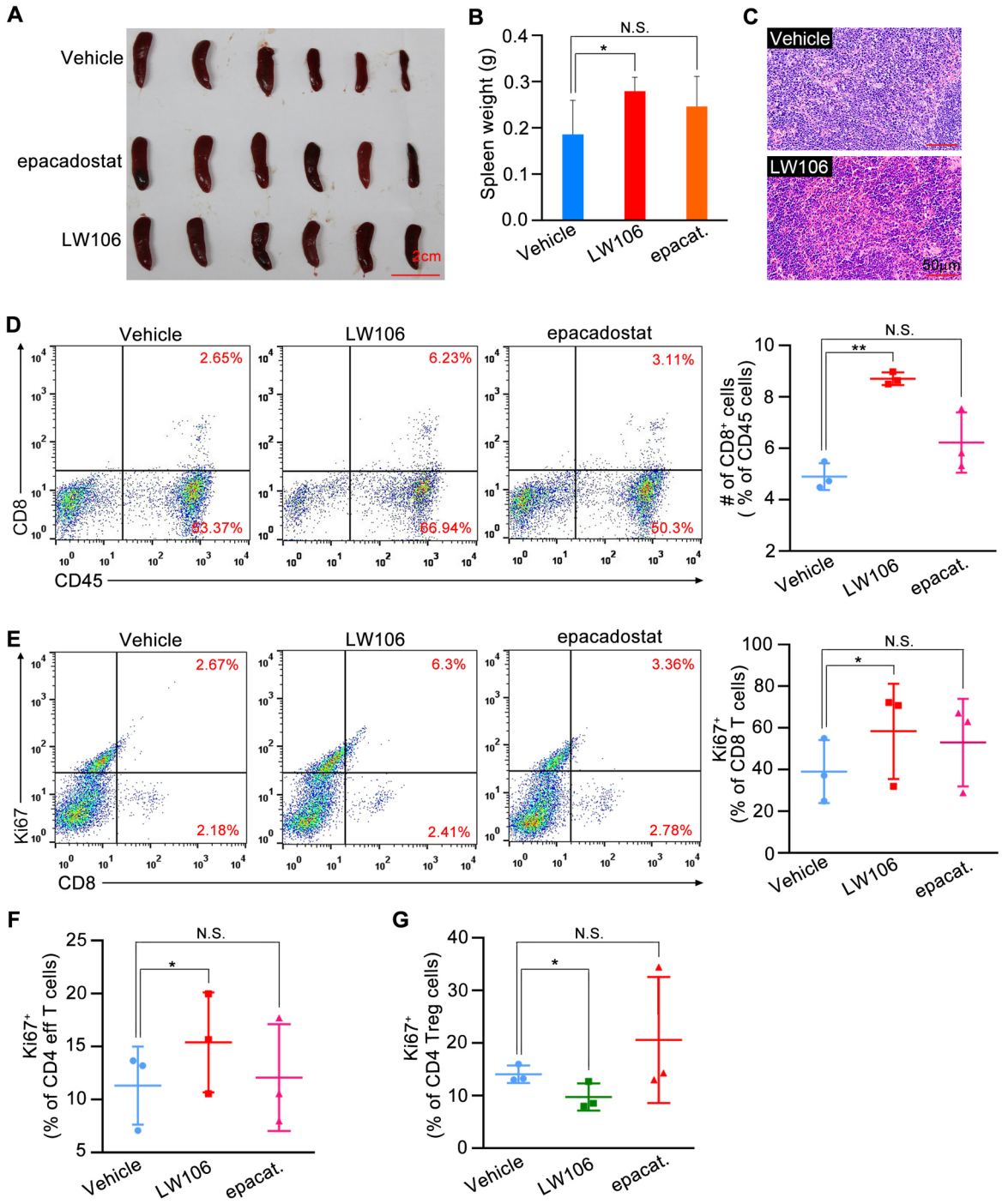

BPH_14351_F5.jpg

Fig. 6

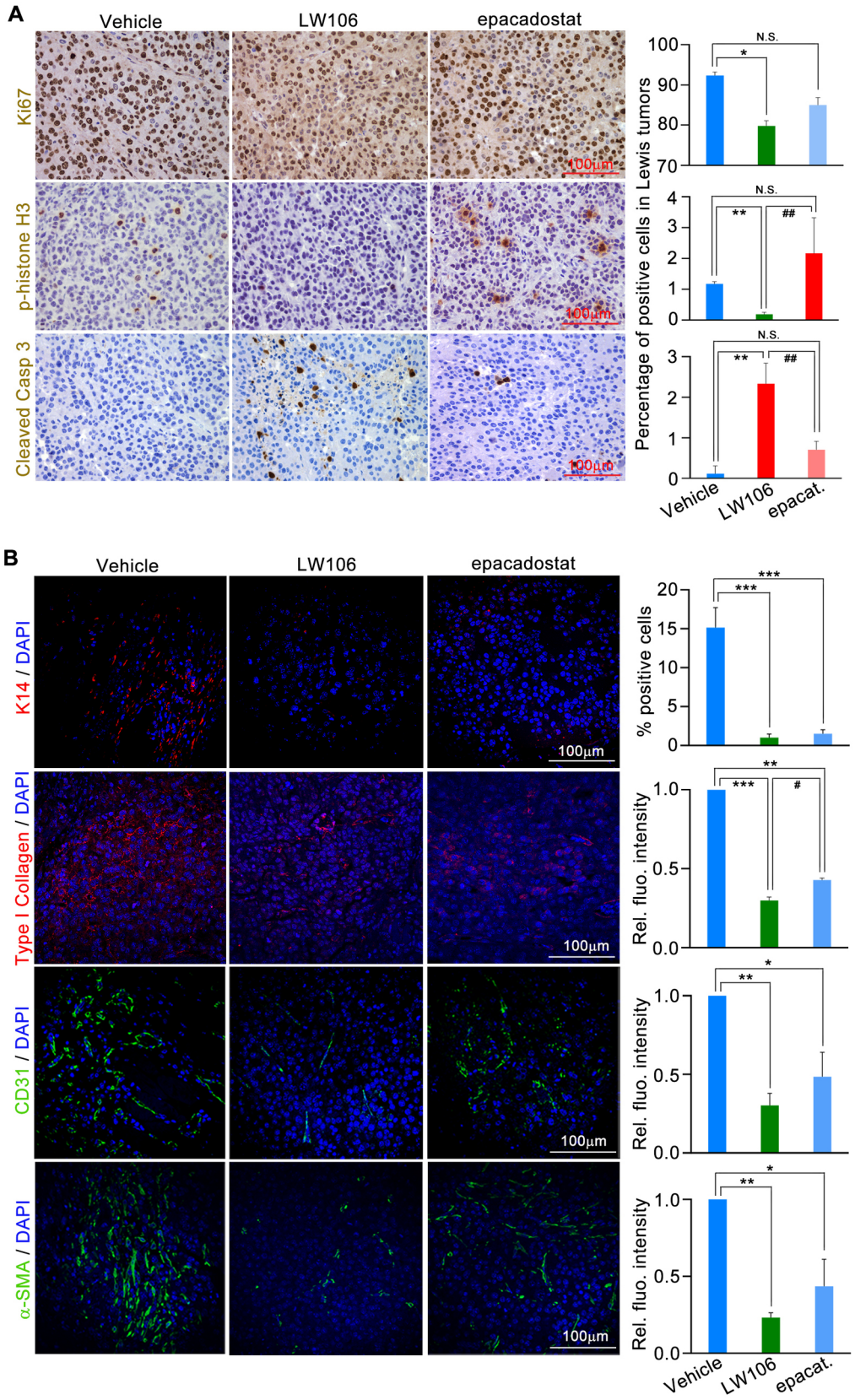

BPH_14351_F6.jpg

Fig. 7

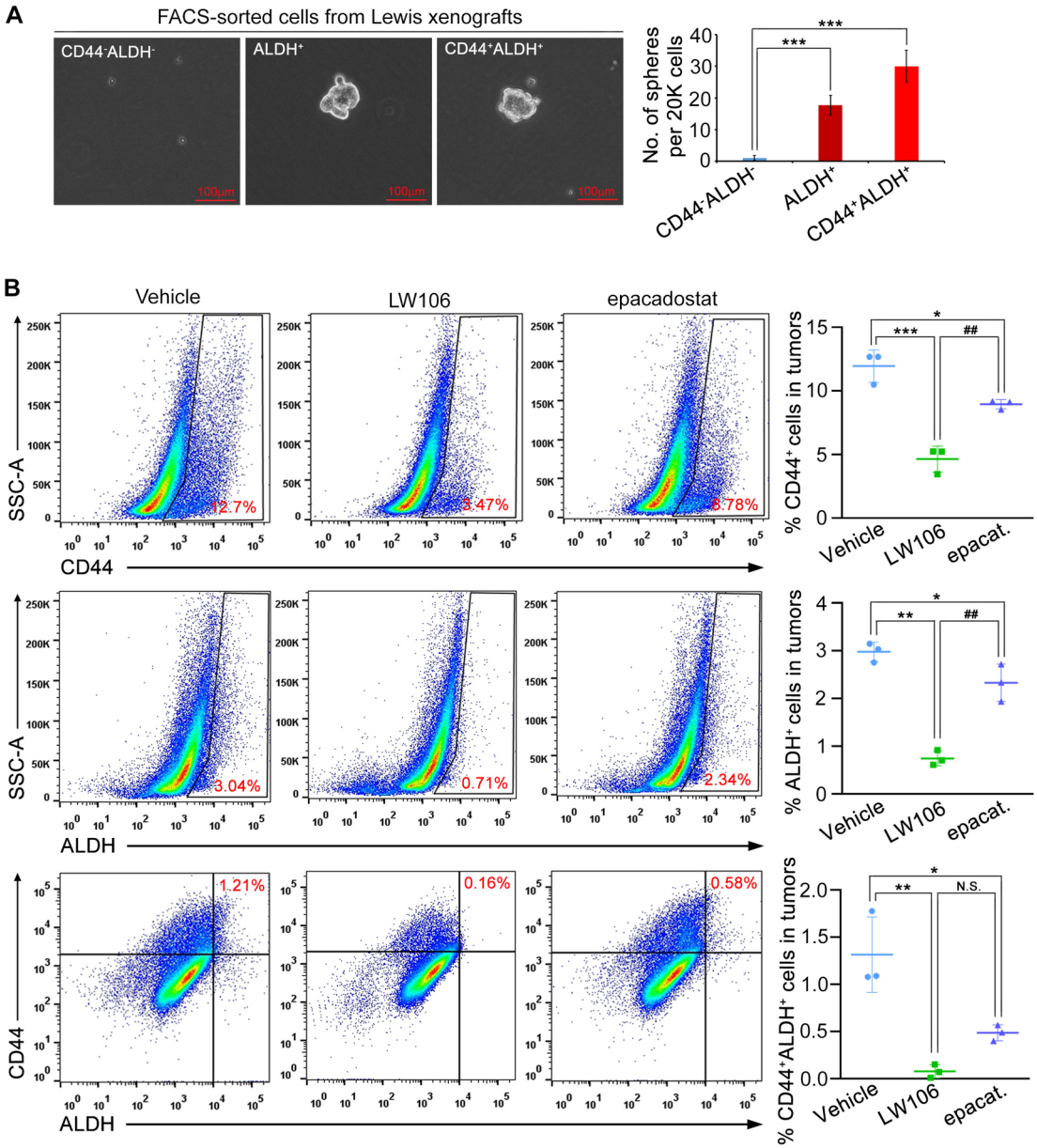

BPH_14351_F7.jpg